

Ring-Opening Reaction of 1-(*N,N*-Dimethylcarbamoyl)pyridinium Chloride with Hydroxide. A Model for the Alkaline Diphosphopyridine Nucleotide Reaction*

S. L. Johnson† and K. A. Rumon

ABSTRACT: 1-(*N,N*-Dimethylcarbamoyl)pyridinium chloride, I, in alkaline solutions produces 5-(3,3-dimethyl-1-ureido)-2,4-pentadienal, IV, which is the Schiff base of 1,1-dimethylurea and 5-hydroxy-2,4-pentadienal (glutacondialdehyde). Compound IV has two acid dissociation constants the values of which are $10^{-12.0}$ and $10^{-1.78}$. The rate of formation of IV is dependent upon $[\text{OH}^{-2}]$ and $[\text{B}][\text{OH}^{-}]$, where B is a general base. These

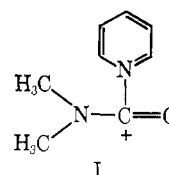
data are consistent with the formation of the pseudobase from I followed by a rate-limiting base-catalyzed ring-opening reaction to form IV. Compound IV decomposes to glutacondialdehyde and 1,1-dimethylurea at low and very high pH, and to pyridine and dimethylamine at intermediate pH. The latter reaction has a bell-shaped pH-rate profile with a rate maximum at pH 11.8.

DPN and its analogs undergo poorly defined chemical changes in alkaline solutions which are characterized by the production of materials which absorb visible or near ultraviolet radiation (Kaplan *et al.*, 1951). DPN also interacts with a large number of enzymes to form near ultraviolet-absorbing complexes (Racker and Krimsky, 1952; Theorell and Yonetani, 1964). The nature of these DPN-enzyme interactions has not been elucidated, although charge transfer complexing and 4-addition have been proposed mainly on the basis of spectral observations (Kosower and Klinedinst, 1956; Kosower, 1956; Van Eys and Kaplan, 1957). In this and following papers we will demonstrate that ring opening readily takes place with DPN analogs. The spectral properties of the ring-opened products are very similar to 1,2- or 1,4-dihydronicotinamide derivatives.

The alkaline DPN reaction is characterized by the production of an intermediate absorbing at 3420 Å which is subsequently transformed to a fluorescent final product which absorbs at 3600 Å. The alkaline fluorescence of DPN is used as an analytical tool in biochemical research (Lowry *et al.*, 1957). This reaction takes place only at higher pH values and at the expense of a ribose-nicotinamide cleavage reaction (Kaplan *et al.*, 1951), which strongly suggests that the production of chromophoric products is higher order in hydroxide ion than the ribose-nicotinamide cleavage, which is first order in hydroxide (Anderson and Anderson, 1963).

In the following papers we have shown that pyridinium compounds containing electron-withdrawing substituents are susceptible to nucleophilic reactions with hydroxide at the 2-position of the ring with subsequent ring opening. It is

expected that other nucleophiles containing two ionizable hydrogens at the nucleophilic atom such a lysine would behave in a similar fashion. The alkaline reaction with the 1-(*N,N*-dimethylcarbamoyl)pyridinium ion, I, described in this paper has been investigated in greater detail than the reactions of the other DPN analogs because of the ease of identification of the symmetrical final products by nuclear magnetic resonance spectrometry. This ring-opening reaction is believed



to be slowly reversible, because of the nature of the decomposition reaction of the ring-opened form and because of analogies with other pyridinium systems to be described. A future paper will describe the extremely facile ring-opening reaction of 1-(*N,N*-dimethylcarbamoyl)nicotinamide cation which ring opens with a rate constant 10^5 greater than that for I. Furthermore the fluorescent final product from this reaction has identical chemical and physical properties as the final DPN alkaline product. Also to be described is the reversible alkaline ring-opening reactions of the 1-*N*-methyl derivatives of nicotinamide and 3-acetylpyridine.

Results

Formation of IV from I. The rate of formation of the intermediate IV in buffered water solutions was measured at 3400 or 4100 Å, depending upon the pH. Figure 1 is a typical intensity-time plot showing the rapid formation of IV. In alkaline solutions the formation rate is much greater ($>200\times$) than the decomposition rate, so that first-order kinetic plots of IV formation are justifiable, assuming that the

* From the Mellon Institute, Pittsburgh, Pennsylvania 15213, and Department of Biochemistry, University of Pittsburgh School of Medicine, Pittsburgh, Pennsylvania 15213. Received September 9, 1969. This investigation was supported in part by Public Health Grant GM 11834-02 from the National Institutes of Health.

† Present address: Department of Biochemistry, School of Medicine, University of Pittsburgh, Pittsburgh, Pennsylvania 15213.

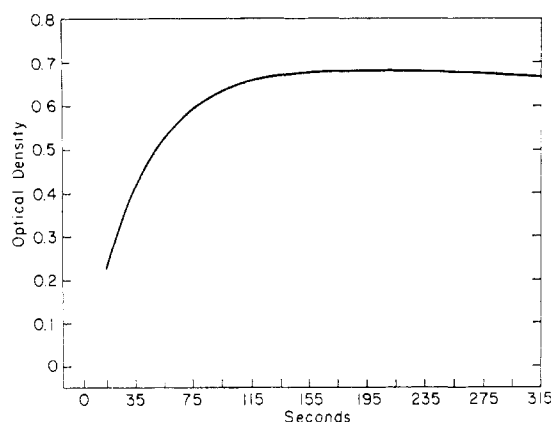
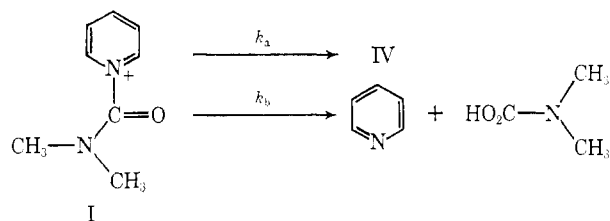


FIGURE 1: Optical density (OD_{obsd}) vs. time at 3400 Å resulting from the addition of 4.96×10^{-4} M I to a 0.165 M phosphate buffer, $\mu = 0.6$, at pH 10.59.

maximum optical density, OD_{max} , is equal to the hypothetical infinity time optical density, OD_{∞} . The observed rate constants for the formation of IV and disappearance of I as followed at 2600 Å are exactly identical, indicating that IV is being formed from I, not from some unsuspected impurity in I. The formation of IV from I may be described by the following equations.



$$-\frac{d[I]}{dt} = (k_a + k_b)[I] \quad (1a)$$

$$[I] = [I_0]e^{-(k_a + k_b)t} \quad (1b)$$

$$\frac{+d[IV]}{dt} = k_a[I] = k_a[I_0]e^{-(k_a + k_b)t} \quad (2a)$$

$$[IV] = \frac{k_a}{k_a + k_b}[I_0](1 - e^{-(k_a + k_b)t}) \quad (2b)$$

$$-\frac{d[C_5H_5N]}{dt} = k_b[I] = k_b[I_0]e^{-(k_a + k_b)t} \quad (3a)$$

$$[C_5H_5N] = \frac{k_b}{k_a + k_b}[I_0](1 - e^{-(k_a + k_b)t}) \quad (3b)$$

The yield ratio at any time of $[IV]:[C_5H_5N]$ is $k_a:k_b$, the ratio of eq 2b and 3b. The infinity-time yield of IV is therefore equal to $[I_0]k_a/(k_a + k_b)$, where $[I_0]$ is the initial concentration of I, and the observed rate coefficient of formation of IV or disappearance of I is equal to $k_a + k_b$.

The amount of IV formed from I is pH dependent and was determined as follows: the initial optical density of IV formed

by adding I to solutions of various pH was determined by extrapolating to zero time on first-order plots at 3400 or 4100 Å for those solutions in which IV is immediately formed and then decomposes slowly. The maximum optical density was taken (Figure 1) for those solutions in which IV is slowly formed. The optical density corrected for the ionization of IV ($pK_a = 12$; see the Experimental Section) and divided by the initial concentration of I gives an apparent initial extinction coefficient value ϵ' for IV proportional to the initial concentration of IV formed from I at various pH values as seen in Figure 2. The leveling off of ϵ' at high pH is not due to limited solubility of IV as the ϵ' value is independent of the initial concentration of I. The same ϵ' value is also obtained in rigorously deoxygenated solutions to which I is added.

The plot of $\log \epsilon'$ vs. pH in Figure 2a is linear at lower pH with a slope of 0.91. At pH higher than 13 in Figure 2b the value is invariant indicating that 100% IV is formed in this region. The rate of formation of IV is second order in hydroxide by the following argument. Because pyridine is formed in nearly 100% yield from I at pH < 11.4 therefore eq 4 holds, where the rate of formation of IV, $k'_{\text{obsd}} = k_b$. Since it follows from the yield data at pH < 11.4

$$\frac{[IV]_{\infty}}{[C_5H_5N]_{\infty}} = \frac{k_a}{k_b} \sim \frac{k_a}{k'_{\text{obsd}}} \sim \frac{\% [IV]_{\infty}}{100} \propto \epsilon' \quad (4)^1$$

that $k_b > k_a$, then $k'_{\text{obsd}} \sim k_b$. The rate constant k_b has previously been determined and is equal to $k_{\text{OH}}[\text{OH}^-]$, where k_{OH} is $1.67 \text{ M}^{-1} \text{ min}^{-1}$ (Johnson and Rumon, 1965). Because the yield of IV is first order in hydroxide, the rate constant for formation of IV must be second order in hydroxide in order to give the linear log yield-pH dependence with the near unity slope seen in Figure 2. Therefore $k_a = k'_a[\text{OH}^-]^2$.

The data in Figure 2 can be analyzed quantitatively in the following fashion: eq 5 holds at higher pH values where the yield of IV levels off, as well as at lower pH values.

$$\frac{[IV]_{\infty}}{[I]_0 - [IV]_{\infty}} = \frac{k'_a[\text{OH}^-]}{k_{\text{OH}}} \quad (5)$$

From this relationship the yield of IV as a function of pH and initial I concentration can be obtained (eq 6, where ϵ_{IV} is the extinction coefficient of IV).

$$[IV]_{\infty} = \frac{[I]_0}{\frac{k_{\text{OH}}}{k'_a} \times \frac{[H^+]}{K_w} + 1} = \frac{\epsilon' [I]_0}{\epsilon_{\text{IV}}} \quad (6)$$

Therefore

$$\epsilon' = \frac{\epsilon_{\text{IV}}}{\frac{k_{\text{OH}}}{k'_a} \frac{[H^+]}{K_w} + 1} \quad (7)$$

A plot of $1/\epsilon'$ vs. $[H^+]$ should give a straight line with an intercept equal to $1/\epsilon_{\text{IV}}$ and a slope equal to $1/\epsilon_{\text{IV}} \times k_{\text{OH}}/k'_a$

¹ k'_{obsd} refers to the observed rate of formation of IV. k_{obsd} refers to the observed rate of decomposition of IV.

$k'_a K_w$. The data in Figure 2a,b give linear plots with values of 34,500 mole⁻¹ cm⁻¹ and 72,700 M⁻¹ cm⁻¹ for the extinction coefficient of IV at 3400 and 4100 Å, respectively. These quantities agree within 5% with the extinction coefficients obtained by placing preformed IV in buffers where IV is either completely protonated or completely ionized. The value of k'_a/k_{OH} from the plots range from 25 to 78 mole⁻¹, with a mean value of 65 M⁻¹. The value of k'_a then is 1.1×10^2 M⁻² min⁻¹.

A buffer concentration effect was noticed in the optical density due to IV when I is placed in buffer solutions. OD_{max} increases with increasing buffer concentration when identical amounts of I decompose in a set of carbonate and phosphate buffers of increasing concentration, but identical pH within the series. In the case of the carbonate buffers the rate of formation of IV was slow enough to permit rate data to be obtained at a number of pH values. A plot of $OD_{max} \times k_{obsd}$ vs. PO_4^{3-} or CO_3^{2-} is linear. A plot of the slopes from the carbonate slopes vs. OH^- is linear. This indicates that the value of k_a in eq 4 is given by

$$k_a = k'_a[OH^-]^2 + k''_a[CO_3^{2-}][OH^-] \quad (8)$$

Properties of IV. The various properties of IV were studied with a preparation made *in situ* or with a dried preparation containing only inorganic salt impurities. The structure proposed for IV is the Schiff base of 1,1-dimethylurea and glutacondialdehyde. The properties of IV are as follows. In very acid solution IV is protonated (probably on the carbamoyl oxygen) and absorbs maximally at 3925 Å, ϵ 53,000 M⁻¹ cm⁻¹; over most of the pH range IV is neutral and absorbs maximally at 3350 Å, ϵ 34,000 M⁻¹ cm⁻¹; in very alkaline solution IV is anionic (III) and absorbs maximally at 4100 Å, ϵ 72,000 M⁻¹ cm⁻¹. With the aid of the absorption properties of IV, two pK values were determined: $pK_b = -1.78$, and $pK_a = 12.0$. The infrared spectrum of anionic IV has strong bands at 1615 and 1592 cm⁻¹. These bands are consistent with the Schiff base structure proposed for IV. For comparison, the sodium salt of glutacondialdehyde has a single intense band at 1595 cm⁻¹ in the carbonyl stretching region. Polarographic reduction of IV at pH 7.2 takes the form of a double wave with half-wave potentials at -1.65 and -1.97 V vs. saturated calomel electrode. This result is consistent with an aldehyde and Schiff base structure for IV. Glutacondialdehyde has a single half-wave reduction potential at -1.87 V under these conditions. The proton magnetic resonance signals of anionic IV occur in three main complex groups in the =CH region: a set of four lines from -449 to -420 cps from the *t*-butyl alcohol standard in D₂O, a set of three lines from -394 to -366 cps, and a set of four lines from -296 to -259 cps. Neutral IV has four main groups of signals in the =CH region: a doublet at -542 and -537 cps, a group of five lines from -512 to -489 cps; a group of four lines from -481 to -461 cps, and a group of six lines from -408 to -377 cps. Compound IV has one methyl signal at -104 cps in both its anionic and neutral forms, and at -109 cps in its protonated form. The anionic IV proton magnetic resonance signals may be compared with those of anionic glutacondialdehyde, VI, which occur as a doublet at -441 cps ($J = 10$ cps) due to the aldehydic protons; a triplet at -382 cps ($J = 13$ cps) due to the C₃ proton; and four signals at -273, -268, -264, and -254 cps due to the C₄ (C₂) protons split by both C₃ and

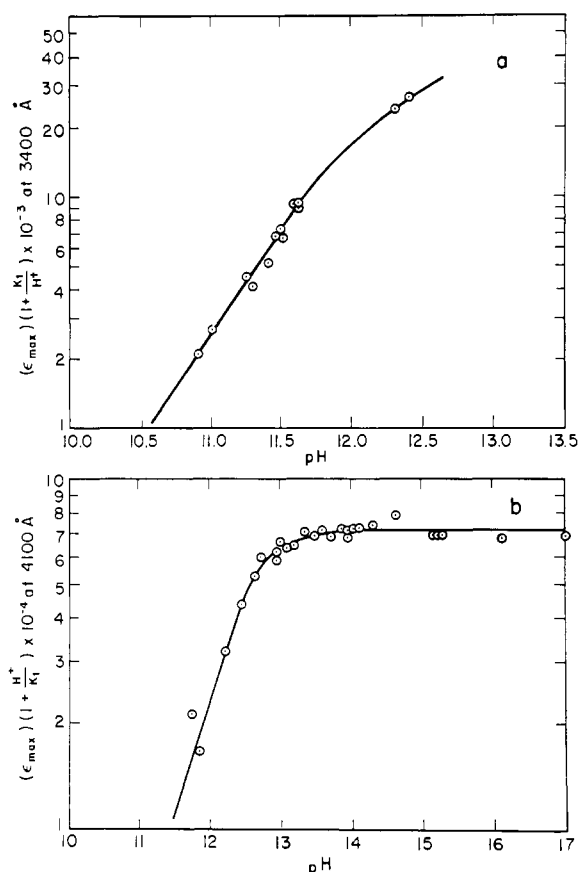
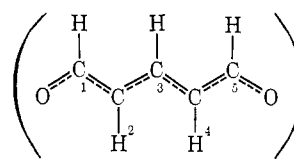


FIGURE 2: Dependence of yield concentration of IV from I: (a) $(\epsilon_{max})(1 + K_1/[H^+])$ for the neutral species (3400 Å) and (b) $(\epsilon_{max}) \cdot (1 + [H^+]/K_i)$ for the anionic species (4100 Å). ϵ_{max} is OD_{max} or OD_0 divided by the initial concentration of I.

aldehyde protons. The relative areas of the three groups of signals are 2:1:2 in accordance with their assignment.



VI

The decomposition products of IV are pH dependent. Glutacondialdehyde and *N,N*-dimethylurea, path c (Scheme I), are major products at very high pH (>13.5) or at low pH (<5), whereas pyridine and dimethylamine, path d, are major products at intermediate pH (7–13). In very alkaline solutions glutacondialdehyde can be isolated from the reaction mixture.

A pictorial indication that IV is decomposing by two paths is seen in repeated wavelength scans of alkaline solutions to which I has been added (Figure 3). At pH 13, where IV is instantly formed, the decomposition of IV yields the final glutacondialdehyde band which is much smaller than the original IV band. At higher pH values the intensity of the final glutacondialdehyde band approaches the intensity of the

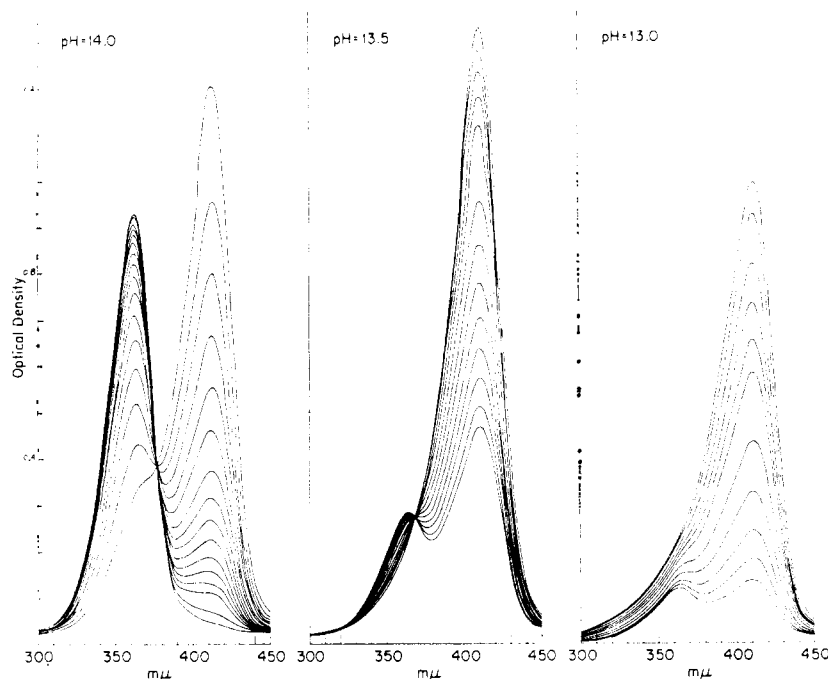


FIGURE 3: Scanned spectra of reacting solutions of IV at various pH values. The first reading was taken at *ca.* 15–30 sec after IV was added to the alkaline solutions.

original IV band, indicating that higher yields of glutacondialdehyde are obtained at higher pH. The low intensity of the final glutacondialdehyde band at pH 13 is not due to instability at this pH, as determined by stability measurements on authentic glutacondialdehyde, or to a change in the ionization state of glutacondialdehyde in the pH region of 13 and above, as glutacondialdehyde has a *pK* of 5.75 (Schwarzenbach and Lutz, 1940) or to a change in the ionization state of IV. The position of the isosbestic point varies with pH as follows: 0.5 M KOH, 3680 Å; 1.0 M KOH, 3740 Å; 2.0 M KOH, 3750 Å; 5.0 M KOH, 3770 Å; 10.0 M KOH, 3775 Å. In 0.1 M KOH so little glutacondialdehyde is formed from IV that no isosbestic point is obtained. Both IV and glutacondialdehyde are fully ionized in these solutions; therefore equilibrium between the acid and base forms of these materials should not affect the isosbestic behavior. If IV decomposes by concurrent kinetics

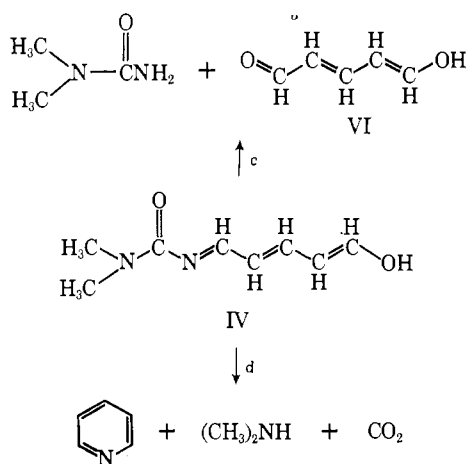
to glutacondialdehyde (G) and a transparent material (L), and if the ratio [L]:[G] at any time is *x*, which is constant at constant pH, then an isosbestic condition is obtained. This condition is obtained when $\epsilon_G = \epsilon_{IV}(1 + x)$. Therefore the optical density equals $\epsilon_{IV}([G] + [G]x + [IV]) = \epsilon_{IV}C_t$, where C_t is the total concentration of all three components of the reacting mixture. The higher *x* is, that is, the lower the yield of glutacondialdehyde from IV, the lower the wavelength at which the isosbestic point will occur. It is proposed that L is pyridine, which does not absorb in the 3600–3800 Å region.

Total Yields of Products from 1-(*N,N*-Dimethylcarbamoyl)-pyridinium Chloride. In Figure 4 are shown the final yields of glutacondialdehyde and pyridine from the decomposition of I in solutions of various pH. For comparison, the yield of the intermediate IV (from which arise glutacondialdehyde and pyridine) is also shown. All products were determined by ultraviolet spectrophotometry. Gas-liquid partition chromatography and nuclear magnetic resonance analysis of pyridine confirmed the ultraviolet spectrophotometric results. It is to be noted that in alkaline solutions where 100% IV has been formed the increase in yield of glutacondialdehyde from IV with pH exactly parallels the decrease in yield of pyridine.

Kinetics of Decomposition of IV. The decomposition kinetics of IV were studied spectrophotometrically over a very wide pH range as shown in Figure 5. These kinetics were accurately first order to 90% reaction. Identical rate constants were obtained for identical runs at 3400 and 4100 Å over the pH range 11–13, and at 3400 and 3950 Å in the very acid pH regions.

In solutions of pH < 6 general catalysis was found for the decomposition of IV in acetate and formate buffers. The kinetics in the acetate buffers were studied at six different buffer ratios, $x = [\text{OAc}^-]:[\text{HOAc}]$, ranging from 10 to 0.33. A plot of $(k_{\text{obsd}}^d - k_h[\text{H}^+])/[\text{HOAc}]$ vs. *x* (where k_h is the

SCHEME I



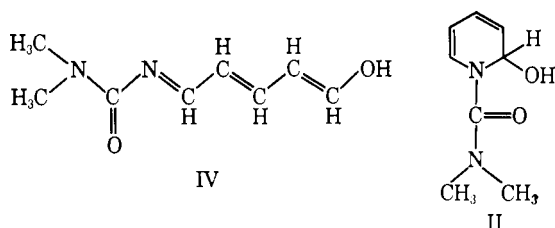
catalytic coefficient for hydrogen ion catalysis below pH 6) yields k_{HOAc} as the slope and k_{OAc} as the intercept. The two buffer terms are approximately equal in magnitude: $25 \times 10^{-6} \text{ M}^{-1} \text{ min}^{-1}$ and $17 \times 10^{-6} \text{ M}^{-1} \text{ min}^{-1}$, respectively.

The solid line in Figure 5 was calculated from the following equation.

$$k = \frac{3.61}{1 + \frac{60.3}{[\text{H}^+]} + \frac{6.03 \times 10^{-4}}{[\text{H}^+]^2}} + 7.0 \times 10^{-6} + \frac{82.6 \times 10^{-14}}{(2.51 \times 10^{-12} + [\text{H}^+]) \left(1 + \frac{10^{-12}}{[\text{H}^+]} + \frac{[\text{H}^+]}{60.3}\right)} + \frac{1.5 \times 10^{-16}}{[\text{H}^+] + \frac{[\text{H}^+]^2}{10^{-2}} + \frac{[\text{H}^+]^3}{6.0 \times 10^{-11}}} \text{ min}^{-1}$$

Discussion

The interaction of hydroxide with 1-(*N,N*-dimethylcarbamoyl)pyridinium chloride results in a ring-opening reaction to produce an unstable intermediate, as well as in a nucleophilic displacement of pyridine from the carbonyl carbon. The reasons for postulating that the product formed at higher pH values results from ring opening, IV, rather than from the formation of a pseudobase, II, or from the formation of any other ring addition compound, are enumerated as follows.



The ultraviolet spectrum (3925 Å in its protonated form, 3350 Å in its neutral form, and 4100 Å in its anionic form) is consistent with the ring-opened structure rather than with a ring addition product. The latter would be expected to absorb maximally below 3210 Å in analogy with 1,2-dihydropyridines (Cook and Lyons, 1966).

In acid solutions IV does not revert to I as would be expected of pseudobases.

Glutacondialdehyde and dimethylurea are decomposition products from IV at low or very high pH, indicating that IV is composed of these two fragments, because of the hydrolysis at the imido bond.

The kinetics for the formation of IV indicate that an intermediate is present between I and IV which is most reasonably the pseudobase; therefore IV cannot be the pseudobase. The reason for this is the dependence of the rate of formation of IV on $[\text{OH}^-]^2$. It is difficult to write a reaction path involving two hydroxide ions for the formation of IV from I is given by eq 9, where the first step is a hydroxide addition across the $\text{C}=\text{N}^+-\text{R}$ bond of I and the second step is the general-base-catalyzed ring opening of II, which has its

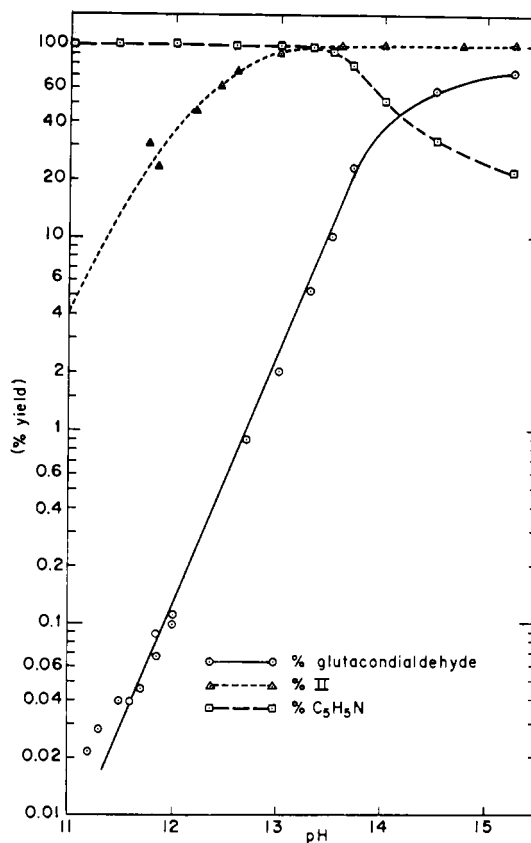
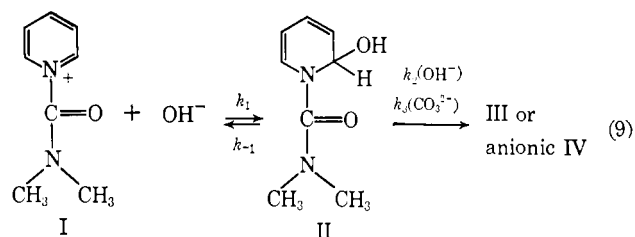


FIGURE 4: Per cent yield of glutacetaldehyde, pyridine, and IV from I as a function of pH.



analogy in the general-base-catalyzed addition of amides and ureas to aldehydes and the reverse reaction (Jencks, 1964). The observed steady-state rate constant for IV formation, k_{obsd}^t , is given by eq 10.

$$k_{\text{obsd}}^t = \frac{k_1 k_2 [\text{OH}^-]^2 + k_1 k_3 [\text{OH}^-] [\text{CO}_3^{2-}]}{k_{-1} + k_2 [\text{OH}^-] + k_3 [\text{CO}_3^{2-}]} \quad (10)$$

If the second step is slow compared to the first, that is, if $k_2 [\text{OH}^-] < k_{-1}$ and $k_3 [\text{CO}_3^{2-}] < k_{-1}$, then

$$k_{\text{obsd}}^t = \frac{k_1 k_2}{k_{-1}} [\text{OH}^-]^2 + \frac{k_1 k_3 [\text{OH}^-] [\text{CO}_3^{2-}]}{k_{-1}} \quad (11)$$

This is the dependence found for the rate of production of IV. An alternate mechanism involving general-base-catalyzed addition of H_2O to I to give IV followed by a specific-base-

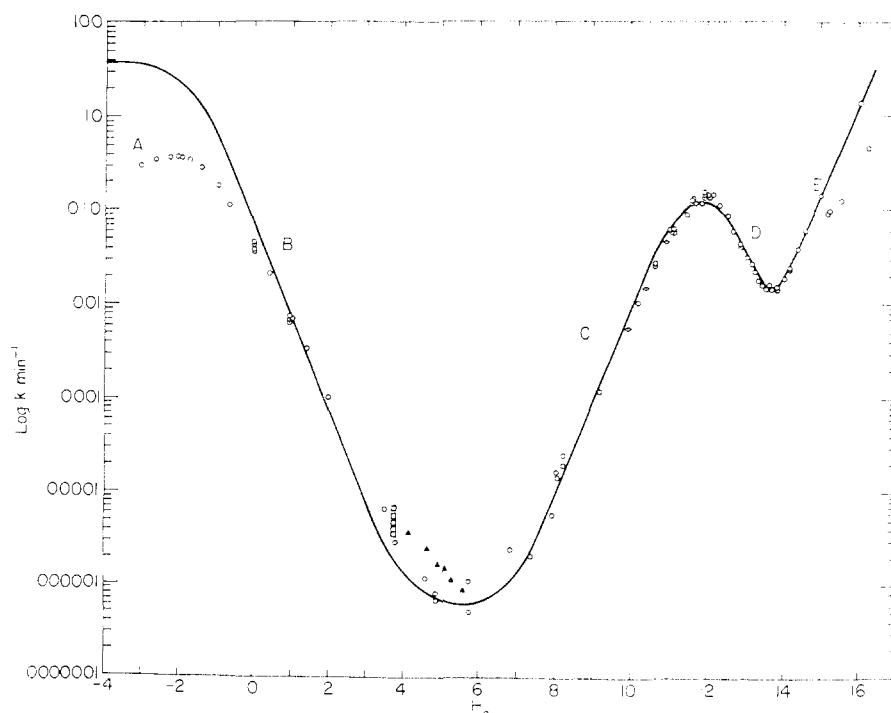


FIGURE 5: Log k_{obsd} vs. pH for the decomposition of IV in aqueous buffer solutions at 25° at $\mu = 0.6$ except for pH < 0.4 and > 13.4 : (○) runs carried in very dilute buffers (< 0.1 M); (□) a series of 1:1 formate buffers of concentrations varying in formate concentration from 0.025 M, 0.05 M, 0.25 M, 0.50 M; the k_{obsd} values increase along this series; (△) a series of 0.5 M- x M acetate-acetic acid buffers where x varies, 0.02 M, 0.01 M, 0.14 M, 0.25 M, 0.50 M, 1.5 M; (◇) in carbonate buffers up to 0.15 M.

catalyzed step does not predict the kinetic dependence on $[\text{OH}^-]^2$ and $[\text{CO}_3^{2-}][\text{OH}^-]$.

The dependence of the rate of the decomposition of IV on pH and the variation of reaction products with pH can be explained by two independent schemes. In Figure 5 the B branch of the pH-rate profile at low pH represents specific-acid- and general-acid-catalyzed Schiff base hydrolysis and the E branch at very high pH represents specific-base-catalyzed Schiff base hydrolysis. This is because the reaction products at the pH values represented by these two branches are 1,1-dimethylurea and glutacetaldehyde. The C and D branches of the pH-rate profile with the maximum at pH 11.8 represents the formation of pyridine and dimethylamine. Two general paths are consistent with the formation of pyridine and dimethylamine which predict a bell-shaped pH-rate profile: reversal by ring closing to form I followed by hydrolysis at the carbonyl-pyridine bond of I, represented by Scheme II; or by a urea-type hydrolysis of IV, represented by Scheme III. In Scheme II is also included the most probable path for the Schiff base hydrolysis of IV at low and extremely high pH.

At low pH the observed rate constant for the decomposition of IV, $k_{\text{obsd}}^{\text{d}}$, is given by eq 12 from Scheme III. The value of $k_6k_7/(k_{-6} + k_7)$ which best fits the data is 3.61 min^{-1} ,

$$k_{\text{obsd}}^{\text{d}} = \frac{k_6k_7}{(k_{-6} + k_7) \left[1 + \frac{K_b}{[\text{H}^+]} + \frac{K_aK_b}{[\text{H}^+]^2} \right]} \quad (12)$$

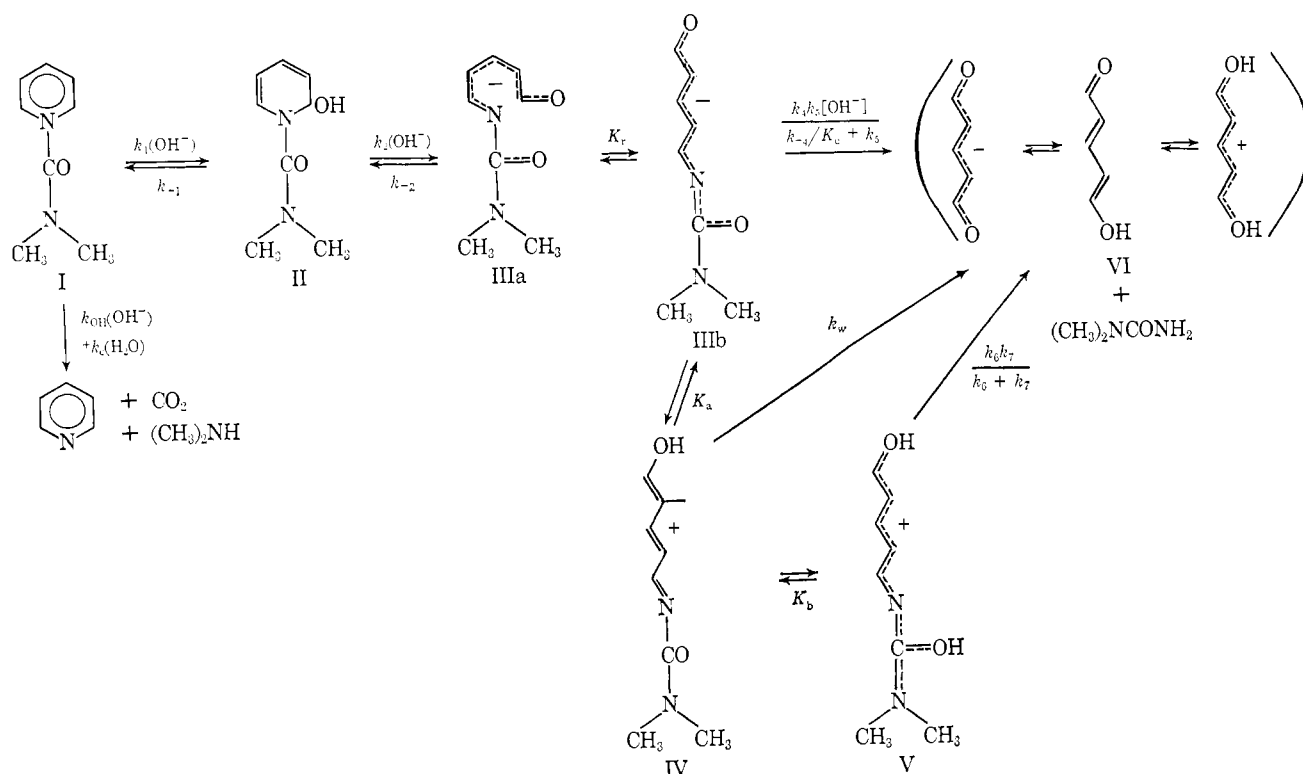
from which the solid line in Figure 5 was calculated. From pH 0 to 4 the observed rate constant is equal to $3.6[\text{H}^+]/$

$K_b = 0.060[\text{H}^+] \text{ min}^{-1}$. The leveling off of the rate constant at pH < 0 and lower is due to the protonation of IV in very acidic solutions. At $-H_0$ values > 1 , the activity of water, an essential component in the reaction, lessens due to the increasing acidic nature of the solution, causing a decrease in the predicted rate constant. The general catalysis found in the B branch of Figure 5 is to be expected for a hydrolytic reaction of a Schiff base (Jencks, 1964). A water term, k_w , equal to $7 \times 10^{-6} \text{ min}^{-1}$ which also represents general acid-base catalysis must be included in order to fit the data in Figure 5.

If the C and D branches of Figure 5 are due mainly to a urea-type hydrolysis according to Scheme III the pH-rate maximum at 11.8 can be accounted for by a two-step mechanism involving first a hydroxide addition to IV to form an anionic tetrahedral intermediate followed by a hydrogen ion catalyzed decomposition of the intermediate. This two-step reaction coupled with the unreactivity of anionic IV which forms at higher pH values accounts for the rate maximum. A simple hydroxide-catalyzed reaction of IV cannot account for the rate maximum. Only a leveling off of the rate constant at higher pH values occurs in such a scheme; no decrease in rate is predicted. Another scheme which involves hydrogen ion catalyzed formation of a neutral tetrahedral intermediate from IV followed by hydroxide ion catalyzed decomposition of the intermediate is also consistent with the data and cannot be excluded. This is so because the leaving group in the case of this amide is considerably more weakly basic than most amide leaving groups which are proton assisted (Johnson, 1967), due to its conjugated enol character.

The rate constant in the C and D branches of Figure 5

SCHEME II



SCHEME III

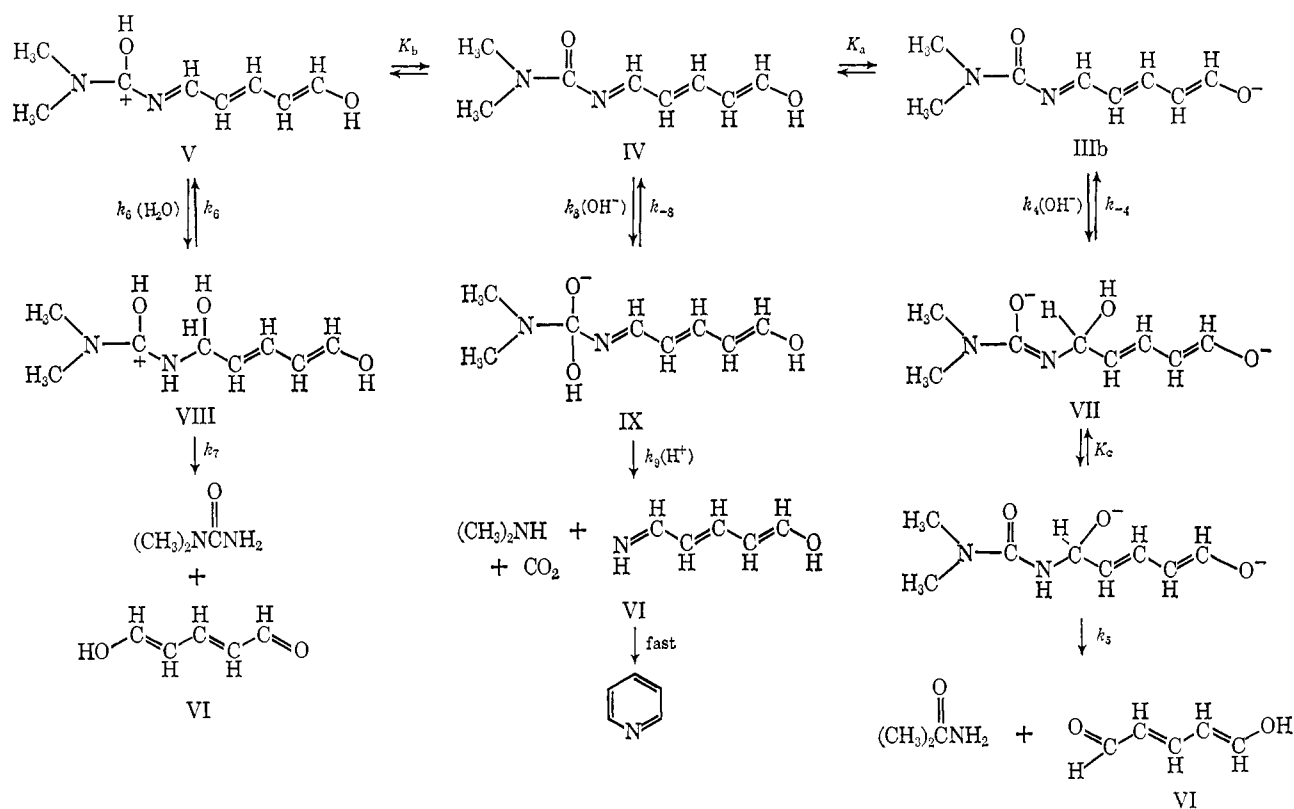


TABLE I: Rate and Equilibrium Constants According to Scheme II.

Entry	Constant	Value	Measurement
1	k_2k_1/k_{-1}	$3.9 \times 10^5 \text{ M}^{-2} \text{ min}^{-1}$	$k_{\text{obsd}}^d/[\text{OH}^-]$ at pH <12
2	k_{OH}	$6.0 \times 10^3 \text{ M}^{-1} \text{ min}^{-1}$	Rate of disappearance of I at pH 6–10 ^a
3	k_{-1}/k_2	$2.15 \times 10^{-3} \text{ M}$ to $4.3 \times 10^{-3} \text{ M}$	Ratio of rate coefficients at pH >13 and pH <11
4	k_1	$0.84\text{--}1.68 \times 10^3 \text{ M}^{-1} \text{ min}^{-1}$	From 1 and 3
5	k_{-2}/K_r	1.11 min^{-1}	From eq 17, low pH behavior, and k_{OH} and k_1
6	$\frac{K_r k_2 k_1}{k_1 k_{-1}} = [\text{III}_b]/[\text{I}][\text{OH}^-]^2$	$3.5 \times 10^3 \text{ M}^{-2}$	From 5 and 1

^a Johnson and Rumon, 1965.

can be expressed in terms of eq 13. At pH values above 7 the $[\text{H}^+]/K_b$ term in the denominator is insignificant. Differentiating k_{obsd}^d with respect to $[\text{H}^+]$ and setting this quantity

$$k_{\text{obsd}}^d = \frac{k_8 k_9 K_w}{(k_{-8} + k_9 [\text{H}^+]) \left(1 + \frac{K_a}{[\text{H}^+]} + \frac{[\text{H}^+]}{K_b} \right)} \quad (13)$$

equal to zero gives the expression for $[\text{H}^+]$ at the pH maximum of 11.8.

$$[\text{H}^+]^2 = \frac{k_{-8}}{k_9} K_a \quad (14)$$

Thus $k_{-8}/k_9 = 10^{-11.6} \text{ M}^{-1}$ upon substituting in the known value of $K_a = 10^{-12.0} \text{ M}$. At pH <12, $k_{\text{obsd}}^d = k_8 [\text{OH}^-] = 73.8 [\text{OH}^-] \text{ min}^{-1}$ and at $14 > \text{pH} > 12$, $k_{\text{obsd}}^d = (k_8 k_9 K_w / k_{-8} K_a) \cdot [\text{H}^+] = 2.90 \times 10^{13} [\text{H}^+] \text{ min}^{-1}$.

In very alkaline solutions the rate constant for the disappearance of IV by a hydroxide-catalyzed Schiff base reaction is given by eq 15. At pH above 14 represented by the

$$k_{\text{obsd}}^d = \frac{k_4 k_5 [\text{OH}^-]}{k_5 + \frac{k_{-4}}{K_e}} \left(1 + \frac{[\text{H}^+]}{K_a} + \frac{[\text{H}^+]^2}{K_a K_b} \right) \quad (15)$$

E branch $[\text{H}^+]/K_a$ and $[\text{H}^+]^2/K_a K_b$ are negligible and k_{obsd}^d reduces to $k_4 k_5 [\text{OH}^-]/(k_5 + k_{-4}/K_e) = 0.015 [\text{OH}^-] \text{ min}^{-1}$. The slight leveling off of the rate at the highest pH values suggests the possibility of hydrogen ion catalysis in the k_5 reaction.

It is interesting to compare the kinetics of IV hydrolysis with that of 5-(2,4-dinitroanilino)-2,4-pentadienal, which was studied from pH 12.7 to 13.7, where only hydroxide catalysis was found (Moss, 1962). The hydroxide catalytic constant in this case is $0.044 \times 10^{-4} \text{ M}^{-1} \text{ min}^{-1}$ at 20°, a factor of 10^4 smaller than the hydroxide catalytic constant of IV.

An alternative scheme for the bell-shaped pH-rate profile for the formation of pyridine and dimethylamine from IV is the return of IV to I and the subsequent hydrolysis of I. Such a scheme is to be preferred over the urea-type hydrolysis

of Scheme III because it is already qualitatively known that glutacodialdehyde derivatives undergo ring closure to form pyridinium compounds with increasing rapidly at higher pH values (Schwarzenbach, 1943). Assuming that steady-state conditions apply to II and I and that the fully extended structure of III, IIIb, is in equilibrium with the coiled structure IIIa as defined by the equilibrium constant $K_r = \text{IIIb}/\text{IIIa}$ which is >1, the decomposition rate of IV is given by eq 16.

$$k_{\text{obsd}}^d = \frac{k_{\text{OH}} [\text{OH}^-] + k_0 k_{-1} k_{-2}}{[\text{OH}^-] [1 + K_r (1 + [\text{H}^+]/K_a)] (k_1 + k_{\text{OH}} (k_{-1} + k_2 [\text{OH}^-] + k_1 k_{-1}))} \quad (16)$$

In the pH range 7–11 the following conditions hold: $[\text{H}^+]/K_a > 1$, $k_{\text{OH}} [\text{OH}^-] > k_0$, and $k_{-1} > k_2 [\text{OH}^-]$. The last condition comes from the principle of microscopic reversibility. Under these conditions eq 16 simplifies to eq 17, which predicts that the rate of disappearance of IV increases with increasing pH, as observed.

$$k_{\text{obsd}}^d = \frac{k_{-2} K_a k_{\text{OH}}}{[\text{H}^+] K_r (2k_1 + k_{\text{OH}})} \quad (17)$$

At pH values greater than 12 the following conditions hold: $[\text{H}^+]/K_a < 1$, and $k_{\text{OH}} [\text{OH}^-] > k_0$. Equation 18 results with these conditions. Because at high pH values a $[\text{H}^+]$ dependence is observed it may be concluded that the constant terms in the denominator of eq 18 are negligible in comparison

$$k_{\text{obsd}}^d = \frac{k_{-1} k_{-2} k_{\text{OH}} / K_r}{2k_1 k_{-1} + k_{-1} k_{\text{OH}} + [\text{OH}^-] k_2 (k_1 + k_{\text{OH}})} \quad (18)$$

with the hydroxide term; therefore eq 19 describes the high pH behavior of IV.

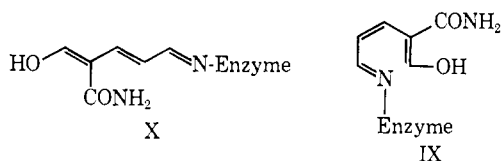
$$k_{\text{obsd}}^d = \frac{k_{-1} k_{-2} k_{\text{OH}} [\text{H}^+]}{K_r K_w k_2 (k_1 + k_{\text{OH}})} \quad (19)$$

The ratio of the high and low pH-rate coefficients as given by eq 19 and 17, respectively, is given by eq 20. Two conditions are possible: (1) when $k_{\text{OH}} > k_1$ the ratio of rate

$$\frac{\text{rate coefficient at pH} > 12}{\text{rate coefficient at pH} < 12} = \frac{k_{-1}(2k_1 + k_{\text{OH}})}{k_2(k_1 + k_{\text{OH}})K_wK_a} \quad (20)$$

coefficients is given by $k_1/k_2K_wK_a$; and (2) when $k_{\text{OH}} < k_1$ the ratio of rate coefficients is given by $2k_{-1}/k_2K_wK_a$. Therefore it is possible to determine k_{-1}/k_2 without being in error by more than a factor of 2. Using the rate coefficients which best fit the rate data of Figure 5 the value of k_{-1}/k_2 is 2.1×10^{-3} M. It can therefore be concluded that $k_2 > k_{-1}$ and that at hydroxide ion concentrations above 4.3×10^{-3} M (or at pH values above 11.6) the k_2 step in Scheme II is no longer rate determining, but rather the k_1 step is rate limiting for the formation of IV from I. Furthermore the rate of IV formation at high pH should be dependent only on the first power of $[\text{OH}^-]$. In Table I are listed various rate and equilibrium constants. Entry 6 is the equilibrium constant between I and the anionic fully stretched form of IV, IIIb. The condition that $k_{\text{OH}} > k_1$, entries 2 and 4, shows that production of I is the rate-determining step in the production of pyridine from IIIb at high pH. Figure 6 demonstrates the energy *vs.* reaction coordinate profile as a function of pH.

If reversal, Scheme III, is the correct path for the decomposition of IV, important biological implications can be made. This storage of DPN in the ring-opened form, X, by an enzyme can be of considerable benefit to DPN by stabilizing it to the



degradation reaction at the nicotinamide-ribose bond. Thus by reversible ring destruction, an advantage is available. Also of importance is the possible role the reversible ring destruction can have in the specificity of a DPN enzyme. In order to form DPN from X it is necessary to form the coiled form of X, XI, which has a shape entirely different from that of X. Substrates can affect greatly the conformation of an enzyme (Koshland and Yankeelov, 1965), which can allow or disallow the folding up of X to XI and then to DPN with its very necessary oxidant properties. This may then be a mechanism of substrate specificity. Of considerable interest is the "alkali stable" DPN of Hilvers *et al.* (1964), which (1) is a stable form of DPN bound to triose phosphate dehydrogenase, (2) is not affected by nucleosidase, and (3) is converted into DPN at lower pH. These properties suggest that "alkali-stable DPN" might be X.

The well-known involvement of the SH group in DPN binding of tightly bound enzyme-DPN complexes can be accommodated in the present hypothesis if the SH group forms a thiohemiacetal type linkage as in XII, thus stabilizing the DPN further and forming a two-point attachment of DPN to its enzyme.

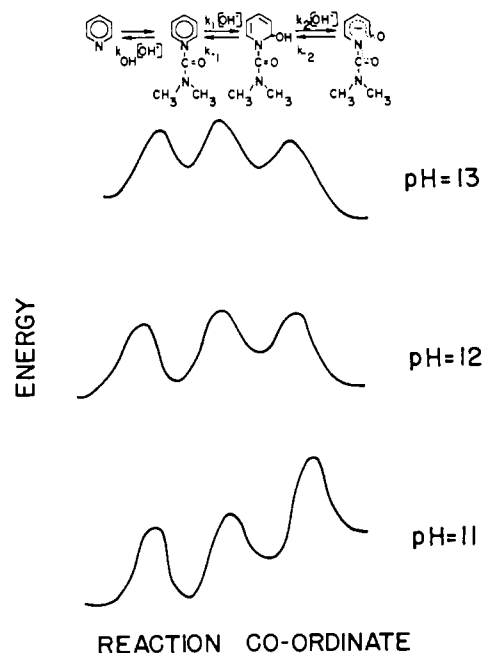
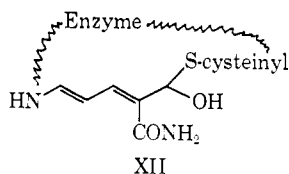


FIGURE 6: Free energy-reaction coordinate profile for the reaction of I and IV as a function of pH.

Experimental Section

Materials. 1-(*N,N*-Dimethylcarbamoyl)pyridinium chloride was prepared as previously described (Johnson and Rumon, 1964). Reagent grade chemicals were used for the preparation of all the buffer solutions. Potassium chloride was added to the buffers to maintain the total ionic strength at 0.6 in the pH range 0.4–13.4. Formate, acetate, diphosphate, Tris, carbonate, triethylamine, carbonate, and triphosphate buffers were used. 1,1-Dimethylurea and tetramethylurea were from K and K Chemical Company.

Glutacondialdehyde was prepared by the method of Schopf *et al.* (1936) from pyridine-sulfur trioxide (Allied Chemical Co.). This material was dried over P_2O_5 for 3 weeks. *Anal.* Calcd for $\text{C}_5\text{H}_5\text{NaO}_2$: C, 50.01; H, 4.18; Na, 19.14. Found: C, 48.63; H, 4.37; Na, 18.71. The absorption coefficient of anionic glutacondialdehyde at 3625 Å is $65,300 \text{ M}^{-1} \text{ cm}^{-1}$. Glutacondialdehyde absorbs maximally at 3670 Å in concentrated HCl, 3000 Å in weakly acid solutions, and 3624 Å above pH 7. In dilute solution (10^{-5} M) glutacondialdehyde is most stable in the pH 11–13 range.

Attempted preparation of the unstable intermediate IV met with limited success. An excess of 50% solution of sodium hydroxide added to a standard solution I at 0° results in a yellow precipitate which has the same ultraviolet and kinetic properties of the unstable intermediate produced in solution. It has no absorption bands in the 2600 Å region where pyridine and I absorb. The sample is not of sufficient purity, being contaminated with sodium chloride, to precisely determine its extinction coefficient. This preparation of IV placed in 5 M HCl has λ_{max} 3925 Å; in 0.1 M HCl, λ_{max} 3350 Å; and in 0.1 NaOH, λ_{max} 4110 Å.

Another preparation method for IV is the titration of a

concentrated solution of I with concentrated sodium hydroxide until I is completely used up, as determined by a rise in pH above 9–10. Extraction of this solution with chloroform yields a brown oil which in 0.1 M HCl solution gives a 3925 Å band and in 0.1 M NaOH gives a 4110 Å band. In 0.1 M NaOH, the 4110 Å band decomposes at the same rate as IV does, and produces glutacondialdehyde in about the same yield. In lieu of working with the prepared intermediates, the intermediate was generated in solution by adding known amounts of I to 0.5 M KOH solution and adding known amounts of this solution to the various buffers in which the kinetics were followed. The amount of intermediate produced in this way is reproducible.

Kinetic Study. For the study of the decomposition of IV, IV was prepared by adding freshly prepared solutions of I of known concentration to 0.5 M KOH and immediately introducing this solution into the various temperature-pre-equilibrated buffers of varying buffer concentration but constant pH. The decrease in optical density was measured with a Beckman D.U. spectrophotometer equipped with a thermostated cell compartment, capable of maintaining constant temperatures to $\pm 0.01^\circ$. Near pH 12, the reaction was followed both at 3400 and 4100 Å; below pH 12, at 3400 Å; above pH 13, at 4100 Å. These solutions were also scanned on a Cary Model 14 spectrophotometer. A plot of $\log (OD_t - OD_\infty)$ vs. time gives straight lines to greater than 90% reaction. From the intercept of this plot the OD_{\max} value was calculated, and the apparent ϵ_0 value was calculated by dividing by the initial concentration of I. The apparent ϵ_0 values were found to be independent of the initial concentration of I, within experimental error. Over the pH range 13–14, the rate of formation of glutacondialdehyde followed at 3635 Å is identical with the decomposition rate of IV.

A kinetic study of the build up of the intermediate is possible since the build up rate is at least 200 times faster than the decomposition rate. A solution of known concentration of I was added to the pre-equilibrated buffer solutions and the optical density at 3400 Å was followed as a function of time. A plot of $\log (OD_{\max} - OD_t)$ vs. time gives a linear plot to greater than 90% reaction. In the same buffers the disappearance of I was followed at 2600 Å, and a plot of $\log (OD_t - OD_\infty)$ vs. time was made. The kinetic constants from the two sets of plots are identical within experimental error under all conditions. In the more basic solutions the decomposition of IV was also studied in the build up experiments. The decomposition of IV followed by adding I directly to the more basic solutions (after IV had been completely formed) followed exactly the same kinetics as the decomposition of preformed IV described in the previous paragraph.

pH Determinations. The runs at acid pH values were made in HCl solutions, from which H_0 values were used (Paul and Long, 1957). Values of pH > 13 were calculated from Harned and Hecker's (1933) activity data for NaOH. In very concentrated NaOH or KOH solutions, acidity functions which had been determined largely from indicator bases consisting mostly of Schiff bases of glutacondialdehyde (Schwarzenbach and Sulzberger, 1944) were used. All other pH values were directly measured on the pH meter. Alkaline solutions measured in this way were prepared with potassium salts in order to avoid electrode error. Under the conditions which were practicable, the ionic strength was maintained at 0.6

with KCl (pH 0.4–13.4). Salt effects were measured separately and found to be small positive effects.

Equilibrium Constants. The ionization constant K_a was determined from data obtained from the quenched kinetic runs as follows: a known amount of I was added to a known volume of 0.5 KOH. A very small aliquot of the resulting solution was immediately added to a buffer solution, and the kinetics were determined in the usual way in the pH 9–15 range. The extrapolated value of OD_0 at zero time was determined at 4100 and at 3400 Å. The pK_a value is equal to $pH + \log (\epsilon_i - \epsilon)/(\epsilon - \epsilon_u)$ at 4100 Å where ϵ_i refers to the extinction coefficient of the completely ionized form of II determined at high pH values, ϵ_u refers to the extinction coefficient of the completely un-ionized form of II determined at low pH values, and ϵ refers to the extinction coefficients observed in intermediate pH values (11–13). Similarly, at 3400 Å, pK_a is equal to $pH + \log (\epsilon - \epsilon_i)/(\epsilon_u - \epsilon)$. Eight determinations at 3400 Å gives $pK_a = 12.09 \pm 0.06$. Nine determinations at 4100 Å gives $pK_a = 11.99 \pm 0.03$. The pK_b values were determined in a similar manner at 3950 Å resulting in $pK_b = -1.78 \pm 0.05$.

Product Studies. When I is added to buffer or KOH solutions with pH values up to 15.2 the yield of pyridine produced is determined by spectral analysis in the 2600 Å region where pyridine absorbs, and from vapor phase chromatographic analysis. The two methods give comparable results.

The transient spectrum of glutacondialdehyde which absorbs at 3600 Å in its protonated form, 3000 Å in its neutral form, and 3625 Å in its anionic form can be seen during the scanning of the spectrum of a reacting mixture of preformed IV in the various buffers. Between the pH range 11–13 glutacondialdehyde in low concentrations is stable enough to be determined spectrophotometrically.

Qualitative product studies by nuclear magnetic resonance analysis were carried out with the use of a Varian A-60 spectrometer. In some experiments I was added to NaOH solutions and the course of the reaction was followed. In other experiments, the solid preparation of IV was added to various buffers and the decomposition of IV followed as a function of time. The signals for authentic pyridine, dimethylurea, and glutacondialdehyde was checked at various pH values.

In very alkaline solutions, the methyl signal for IV at -104 cps (from *t*-butyl alcohol) disappeared as the methyl signal of *N,N*-dimethylurea appeared at -98 cps. Also the characteristic signals of anionic glutacondialdehyde appeared. At pH values lower than 5 the methyl signals of neutral IV (-104 cps) or of protonated IV (-109 cps) disappeared while the methyl signals of 1,1-dimethylurea appeared at -98 cps or at -106 cps in the case of protonated 1,1-dimethylurea.

Dimethylamine and pyridine were detected as major products by nuclear magnetic resonance analysis at pH 9. The rate of appearance of protonated dimethylamine signal at -89 cps paralleled the rate of disappearance of the -104 cps signal of IV. Pyridine was a major product as determined by the appearance of the characteristic pyridine nuclear magnetic resonance spectrum in the reacting solution.

1,1-Dimethylurea was also determined colorimetrically by a modification of an analytical method for urea (Watt and Chrisp, 1954). It was found that the pH conditions for optimal analysis of 1,1-dimethylurea are different from those for urea. Using a solution of 0.5 M *p*-dimethylaminobenzaldehyde in 1.2 M HCl, 10^{-2} M 1,1-dimethylurea can be observed

as its Schiff base of *p*-dimethylaminobenzaldehyde, absorbing at λ_{\max} 4200 Å. Unfortunately glutacondialdehyde at the same concentration interfered somewhat with a quantitative determination of 1,1-dimethylurea, but a qualitative determination was still possible. When a 10^{-1} M solution of IV decomposed in 1.0 M NaOH, and the contents of the final solution were analyzed by the *p*-dimethylaminobenzaldehyde reagent, the very characteristic peak at 4200 Å due to 1,1-dimethylurea was present with an optical density corresponding to a 50% yield.

Ammonia was determined by the pyridine-pyrazolone method (Kruse and Mellon, 1953). No interference was found by glutacondialdehyde or 1,1-dimethylurea. When IV was allowed to react in a variety of buffers, pH 11–14, no ammonia could be detected.

References

- Anderson, B. M., and Anderson, C. D. (1963), *J. Biol. Chem.* 238, 1475.
- Cook, N. C., and Lyons, J. E. (1966), *J. Am. Chem. Soc.* 88, 3396.
- Harned, H. S., and Hecker, J. C. (1933), *J. Amer. Chem. Soc.* 55, 4838.
- Hilvers, A. G., Van Dam, K., and Slater, E. C. (1964), *Biochim. Biophys. Acta* 85, 206.
- Jencks, W. P. (1964), in *Progress in Physical Organic Chemistry*, Cohen, S. G., Streitweiser, A., and Taft, R. W., Ed., Vol. 2, New York, N. Y., Interscience.
- Johnson, S. L. (1967), in *Advances in Physical Organic Chemistry*, Gold, V., Ed., Vol. 5, New York, N. Y., Academic, p 237.
- Johnson, S. L., and Rumon, K. A. (1964), *J. Phys. Chem.* 68, 3149.
- Johnson, S. L., and Rumon, K. A. (1965), *J. Amer. Chem. Soc.* 87, 4782.
- Kaplan, N. O., Colowick, S. P., and Barnes, C. C. (1951), *J. Biol. Chem.* 191, 461.
- Koshland, D. E., and Yankeelov, J. A., Jr. (1965), *J. Biol. Chem.* 240, 1593.
- Kosower, E. M. (1956), *J. Amer. Chem. Soc.* 78, 3497.
- Kosower, E. M., and Klinedinst, P. E. (1956), *J. Amer. Chem. Soc.*, 78, 3493.
- Kruse, J. M., and Mellon, M. G. (1953), *Anal. Chem.* 25, 1188.
- Lowry, O. H., Roberts, N. R., and Kapphahn, J. I. (1957), *J. Biol. Chem.* 224, 1047.
- Moss, E. K. (1962), Ph.D. Thesis, University of Arizona, Tucson, Ariz.
- Paul, M. A., and Long, F. A. (1957), *Chem. Rev.* 57, 1.
- Racker, E., and Krimsky, I. (1952), *J. Biol. Chem.* 198, 731.
- Schopf, C. A., Hartman, A., and Koch, K. (1936), *Ber.* 69, 2766.
- Schwarzenbach, G. (1943), *Helv. Chim. Acta* 26, 418.
- Schwarzenbach, G., and Lutz, K. (1940), *Helv. Chim. Acta* 23, 1147.
- Schwarzenbach, G., and Sulzberger, R. (1944), *Helv. Chim. Acta* 27, 348.
- Theorell, H., and Yonetani, T. (1964), *Arch. Biochem. Biophys.* 106, 252.
- Van Eys, J., and Kaplan, N. O. (1957), *J. Biol. Chem.*, 228, 305.
- Watt, G. W., and Chrisp, J. D. (1954), *Anal. Chem.*, 26, 453.